STUDY ON BEHAVIOR OF CONCRETE FILLED ELLIPTICAL STEEL TUBE MEMBERS PART I : SHORT AND LONG COLUMNS UNDER AXIAL COMPRESSION

Xiaoxiong Zha [1, *], Guobin Gong [2] and Xichao Liu [2]

[1] *Shenzhen Graduate School, Harbin Institute of Technology, Shenzhen 518055, China*
[2] *Shenzhen Graduate School, Harbin Institute of Technology, Shenzhen 518055, China*
**(Corresponding author: E-mail: zhaxx@hit.edu.cn)*

Received: 21 September 2011; Revised: 18 January 2012; Accepted: 27 January 2012

ABSTRACT: This paper presents theoretical analysis of concrete filled elliptical steel tube (CFEST) members under axial compression. The theoretical analysis presents the distribution rule of interaction between steel tube and core concrete for CFEST column, which is verified and compared with both experimental tests and finite element (FE) simulations. The assumption of effective confined zone distribution of core concrete is proposed and the influence of cross-section shape on the confinement effect is analyzed. A unified axial compressive strength formula and stability factor are obtained for CFEST columns based on existing formulas for concrete filled circular steel tube (CFCST) columns.

Keywords: Theoretical analysis, Interaction, Concrete filled elliptical steel tube, Axially compressive strength, Stability factor

1. INTRODUCTION

Concrete filled steel tube (CFST) is a composite structure with concrete filled in the steel tube, and if the steel tube is partially filled the CFST is called hollow concrete filled steel tube (HCFST), and if the steel tube is fully filled the CFST is called solid concrete filled steel tube (SCFST). According to the section shapes, CFST can be divided into concrete filled circular steel tube (CFCST), concrete filled elliptical steel tube (CFEST), concrete filled rectangular/square steel tube(CFRST, CFSST) and so on.

Yu et al. [1] proposed a unified formulation to predict composite compressive strength of concrete-filled circular steel tube (CFCST) columns for hollow and solid sections under axial compression based on theory of elasticity. Chitawadagi and Narasimhan [2] studied strength deformation behavior of CFCST under flexure and they examined the effects of steel tube thickness, the cross sectional area of concrete, strength of in-filled concrete and the confinement of concrete on moment capacity and curvature of CFCST. Yang et al. [3] presented testing and analysis of concrete-filled elliptical hollow sections (CFEHS), and they found that the compressive response of CFEHS is sensitive to both steel tube thickness and concrete strength, i.e. higher tube thickness resulting in higher load carrying capacity and enhanced ductility, and higher concrete strengths improving load-carrying capacity but reducing ductility. Dai and Lam [4] proposed a new stress-strain model for the confined concrete for CFEHS member under axial compression, which is validated by finite element simulations. Besides circular and elliptical sections, square hollow sections have been studied by Guo et al. [5, 6]. The effect of eccentricity has been studied by some researchers [7, 8, 9] among others. Unified theory for CFST members is proposed by Zhong [10], in which all the CFST members can be constructed within one framework whether the section is solid or hollow, circular shape or other general shapes.

In the literature, most CFST research is focused on circular sections and axial compressive behavior, and there is little research work for CFEST members [11]. Therefore, the fundamental study of the CFEST can not only fill in the gap in this field, but also provide guidance for practical engineering.

Figure 1 shows a typical CFEST cross section, which has the following characteristics.

- Architectural aesthetics for the elliptical shape cross section and mobile choices of aspect ratios (long side length against short side length).
- Provision of strong and weak axes in an effective manner. For example, for cross sections with equal size in area and with the same material, the major flexural capacity for CFEST member is larger than for CFCST member. In this sense, CFEST will be more economical compared with CFCST under one-way bending and compression.
- Based on the smooth convex characteristic of elliptical cross section compared with round, square and polygonal shaped sections, the elliptical shape can be more effective in reducing the load on the structure caused by fluid. For example, the use of concrete filled elliptic steel tube as bridge pier is more effective in reducing the impact on the pier caused by water flow than the use of concrete filled circular steel tube and rectangular tube [11].

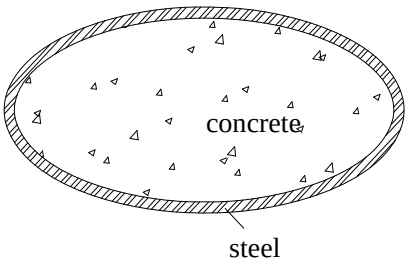

Figure 1. Typical Cross Section of a CFEST Member

In this paper, solid CFEST with steel tube fully filled by concrete will be considered. The paper is followed by section 2 (Stress analysis for the core concrete and external steel tube of CFEST), section 3 (Finite element simulation of short columns under axial compression for CFEST members), and section 4 (Axial compressive strength formula for CFEST short columns), section 5 (Experimental Verification), section 6 (Stability factor under axial compression for CFEST long columns) and section 7 (Concluding remarks).

2. STRESS ANALYSIS FOR THE CORE CONCRETE AND EXTERNAL STEEL TUBE OF CFEST

The analysis of CFEST is divided into two parts: one part is the vertical compressive stress for the steel tube and core concrete respectively, and the second part is the interaction steel tube and core concrete in the horizontal plane. The second part is focused in this paper. The interaction between concrete and steel tube is analyzed according to plane stress consideration, and a unit height is used.

Figures 2(a) and 2(b) show half isolated free body to the symmetrical plane. According to the principle of static equilibrium we have:

$$\sum F_x = 0 \Rightarrow 2N_2 - f_{lx}(0) \cdot 2b = 0 \tag{1}$$

$$\sum F_y = 0 \Rightarrow 2N_1 - f_{ly}(0) \cdot 2a = 0 \tag{2}$$

Solution of (1) and (2) gives：

$$f_{lx}(0) = \frac{N_2}{b},\ f_{ly}(0) = \frac{N_1}{a} \tag{3}$$

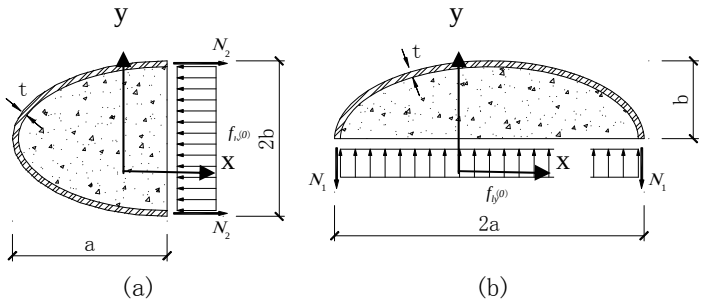

Figure 2. Half Isolated Free Body to the Symmetrical Plane for CFEST

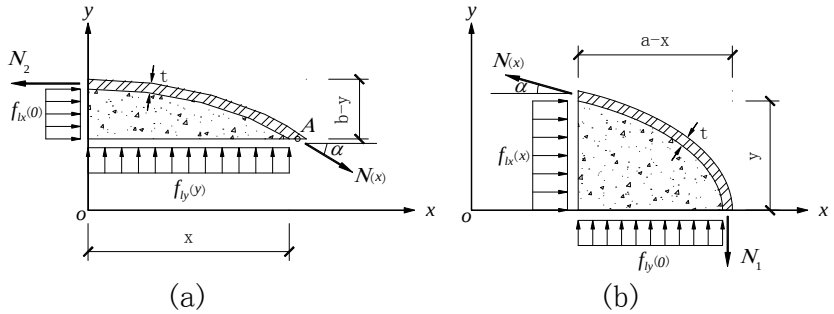

Figure 3. Part of Isolated Free Body for CFEST

Part of isolated free body for concrete filled elliptical steel tube is shown in Figure 3(a) and 3(b). $f_{lx}(x)$ is the lateral pressure of concrete along x when abscissa is x, $f_{ly}(y)$ is the lateral pressure of concrete along y when ordinate is y, $f_{ly}(0)$ is the lateral pressure of concrete along y when ordinate is 0, $f_{lx}(0)$ is the lateral pressure of concrete along x when ordinate is 0, $N(x)$ is circumferential tension of steel tube when abscissa is x, N_1 is circumferential tension of steel tube when abscissa is a , i.e. x=a, N_2 is circumferential tension of steel tube when x=0, α is the angle between x axis and the tangential to the elliptic curve at x. $N(x) = \sigma(x) \cdot t$, $N_1 = \sigma_1 \cdot t$, $N_2 = \sigma_2 \cdot t$, and $\sigma(x)$, σ_1, σ_2 are the circumferential tension of steel tube at x, x=a and x=0 respectively.

According to the principle of static equilibrium we have:

$$\sum F_x = 0 \Rightarrow f_{lx}(0)\cdot(b-y) + N(x)\cdot\cos\alpha - N_2 = 0 \tag{4}$$

$$\sum F_y = 0 \Rightarrow f_{ly}(y)\cdot x - N(x)\cdot\sin\alpha = 0 \tag{5}$$

Taking moment about A, according to $\sum M_A = 0$, we have:

$$f_{lx}(0)\cdot\frac{1}{2}(b-y)^2 + f_{ly}(y)\cdot\frac{1}{2}x^2 - N_2\cdot(b-y) = 0 \tag{6}$$

Since $\tan\alpha = \dfrac{\frac{bx}{a^2}}{\sqrt{1-\left(\frac{x}{a}\right)^2}}$, we have:

$$\sin\alpha = \frac{\frac{bx}{a^2}}{\sqrt{1-\left(\frac{x}{a}\right)^2+\frac{b^2x^2}{a^4}}},\quad \cos\alpha = \frac{\sqrt{1-\left(\frac{x}{a}\right)^2}}{\sqrt{1-\left(\frac{x}{a}\right)^2+\frac{b^2x^2}{a^4}}} \tag{7}$$

Combining the Eqs. 3, 4, 5, 6, 7 we have the solutions as follows:

$$N_1 = \frac{b}{a}\cdot N_2 \tag{8}$$

$$f_{lx} = \frac{N_2}{b} \tag{9}$$

$$f_{ly} = \frac{b}{a^2}\cdot N_2 \tag{10}$$

$$N(x) = \sqrt{1-\left(\frac{x}{a}\right)^2+\frac{b^2x^2}{a^4}}\cdot N_2 \tag{11}$$

As shown in Figure 4, taking the concrete differential element, and taking each of the stresses with orthogonal decomposition and combine along the normal vector $\vec{n}$, we have

$$p(x)\cdot ds = f_{lx}\cdot dy\cdot\sin\alpha + f_{ly}\cdot dx\cdot\cos\alpha \tag{12}$$

$$ds = \sqrt{(dx)^2+(dy)^2} \tag{13}$$

Combining Eqs. 12, 13, we have:

$$p(x) = \frac{\frac{b}{a^2}}{1-\left(\frac{x}{a}\right)^2+\frac{b^2x^2}{a^4}}\cdot N_2 \tag{14}$$

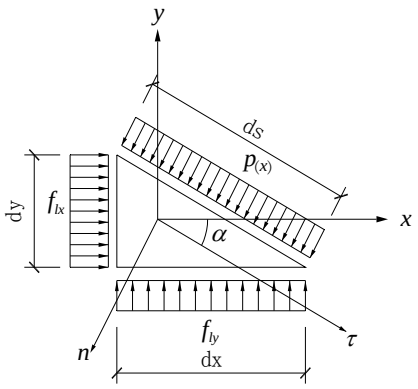

Figure 4. Core Concrete Differential Element

Assuming $a = 142$, $b = 71$, $t = 6$ as an illustrational example, we obtain the resulting circumferential tension of steel tube and the core concrete lateral pressure distribution shown in Figure 5 and Figure 6.

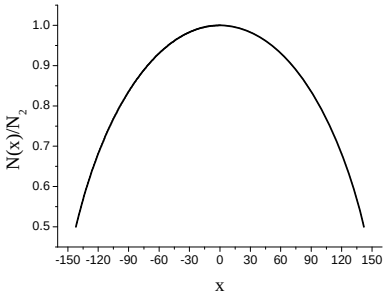

Figure 5. Circumferential Tension of External Steel Tube Along x

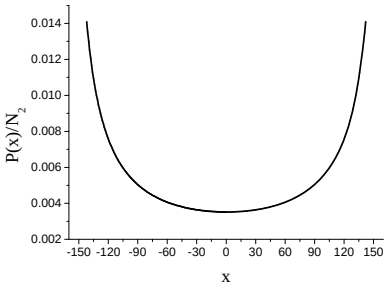

Figure 6. Core Concrete Lateral Pressure Along x

Based on the above theoretical analysis, the distribution of lateral pressure of core concrete in CFEST, is parabolic along the x-axis. The lateral pressure reaches minimum at both ends of short axis of elliptical cross section. The lateral pressure reaches maximum at both ends of long axis of elliptical cross section. The distribution of circumferential tension of external steel tube is parabolic along the x-axis. The circumferential tension reaches maximum at both ends of short axis of elliptical cross section. The circumferential tension reaches minimum at both ends of long axis of elliptical cross section. The distribution of circumferential tensile strain of external steel tube is parabolic along the x-axis. The circumferential tensile strain reaches maximum at both ends of short axis of elliptical cross section. The circumferential tensile strain reaches minimum at both ends of long axis of elliptical cross section.

3. FINITE ELEMENT SIMULATION OF SHORT COLUMNS UNDER AXIAL COMPRESSION FOR CFEST MEMBERS

A general-purpose finite element software ABAQUS is used for simulating CFEST members. Solid elements are used for both steel tube and concrete, and the nodes are tied together, i.e. no sliding. The concrete damaged plasticity model is employed for concrete material, and the details can be found in [12]. The concrete axial compressive stress-strain relation is shown in Figure 7, and the mathematical formulation of expression can be described as follows. More details can be found in [13]

when $\varepsilon \le \varepsilon_e$, $\sigma = E_c\varepsilon$, $E_c = 0.3 f_{ck} / \varepsilon_e$;

when $\varepsilon_e \le \varepsilon \le \varepsilon_c$, $\sigma = f_{ck}\left[\alpha_a\left(\frac{\varepsilon}{\varepsilon_c}\right)+(3-2\alpha_a)\left(\frac{\varepsilon}{\varepsilon_c}\right)^2+(\alpha_a-2)\left(\frac{\varepsilon}{\varepsilon_c}\right)^3\right]$;

when $\varepsilon_c \le \varepsilon \le \varepsilon_u$, $\sigma = f_{ck}\dfrac{\varepsilon/\varepsilon_c}{\alpha_d(\varepsilon/\varepsilon_c-1)^2+\varepsilon/\varepsilon_c}$;

where:

ε_e —compressive strain corresponding to stress with the value of $0.3 f_{ck}$ at hardening stage

ε_c —compressive strain corresponding to stress with the peak value of f_{ck}

ε_c —compressive strain corresponding to stress with the value of $0.5 f_{ck}$ at softening stage

α_a, α_d —model constants

The axial tensile stress-strain relationship is based on energy criterion for concrete, i.e. softened stress-fracture energy relation and the stress-strain curve is shown in Fig. 8, with the mathematical formulation of expression described as follows, G_f and σ_{t0} are concrete fracture energy (the energy required to cause one continuous crack per unit area), and failure stress respectively. When $f_{ck} = 20\text{MPa}$, $G_f = 40\text{N/m}$; when $f_{ck} = 40\text{MPa}$, $G_f = 120\text{N/m}$, and the values of G_f can be obtained using linear interpolation corresponding to other values of f_{ck}. The failure stress σ_{t0} is calculated according to the following formula [14]:

$$\sigma_{t0} = 0.26\times(1.5 f_{ck})^{2/3} \tag{15}$$

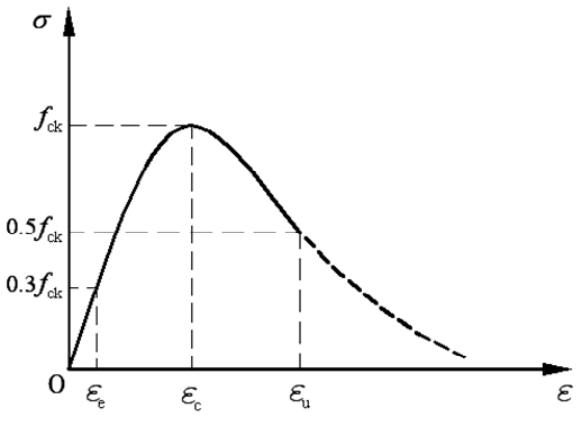

Figure 7. Compressive Stress-strain Relation of Concrete

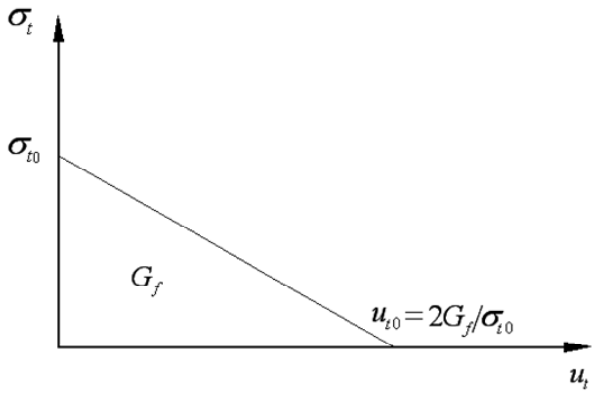

Figure 8. Tensile Softening Model of Concrete

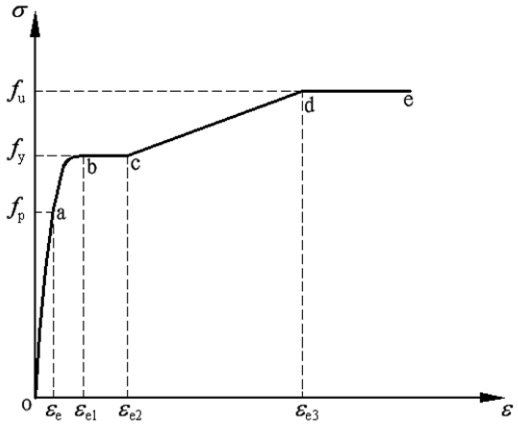

Figure 9. Stress-strain Relation of Steel

Steel axial stress-strain relation is shown in Figure 9, and the mathematical expression can be described as follows [15]:

$$\sigma_s = \begin{cases} E_s\varepsilon_s & \varepsilon_s \le \varepsilon_e \\ -A\varepsilon_s^2 + B\varepsilon_s + C & \varepsilon_e \le \varepsilon_s \le \varepsilon_{e1} \\ f_y & \varepsilon_{e1} \le \varepsilon_s \le \varepsilon_{e2} \\ f_y\left[1+0.6\dfrac{\varepsilon_s-\varepsilon_{e2}}{\varepsilon_{e3}-\varepsilon_{e2}}\right] & \varepsilon_{e2} \le \varepsilon_s \le \varepsilon_{e3} \\ 1.6f_y & \varepsilon_s > \varepsilon_{e3} \end{cases} \tag{16}$$

where,

f_p is proportional limit value of steel

f_y is yield strength value of steel

f_u is ultimate strength value of steel

$\varepsilon_e = 0.8f_y / E_s$, $\varepsilon_{e1} = 1.5\varepsilon_e$, $\varepsilon_{e2} = 10\varepsilon_{e1}$, $\varepsilon_{e3} = 100\varepsilon_{e1}$, $B = 2A\varepsilon_{e1}$,

$A = 0.2f_y / (\varepsilon_{e1} - \varepsilon_e)^2$, $C = 0.8f_y + A\varepsilon_e^{\,2} - B\varepsilon_e$.

and the details can be found in reference [15].

Figure 10 shows an established CFEST finite element model with solid elements for steel and concrete and there are three layers of meshed elements along the steel tube thickness direction.

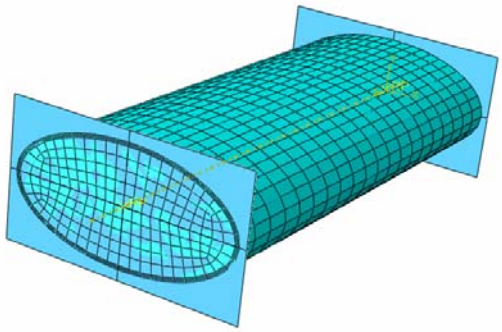

Figure 10. Finite Element Model for CFEST

The boundary condition of the CFEST columns under axial compression is simply supported. The loading condition is by displacement control. For the long column, an initial eccentricity of $e_0 = L/1000$ [16] (L is effective length of the column) along long and short axes of the section is applied.

Figure 11 shows the stress contour for different aspect ratios (long side length against short side length for the cross section) for concrete filled steel tubes modeled by ABAQUS. It can be seen that circular shape is a special elliptical shape with aspect ratio of 1, and its lateral pressure is circlewise uniform. For the elliptical cross section, the lateral pressure is not uniform for core concrete, and changes with the shape of elliptical cross section. The lateral pressure distribution in core concrete is as follows: maximum at both ends of long axis of cross section, minimum at both ends of short axis of cross section.

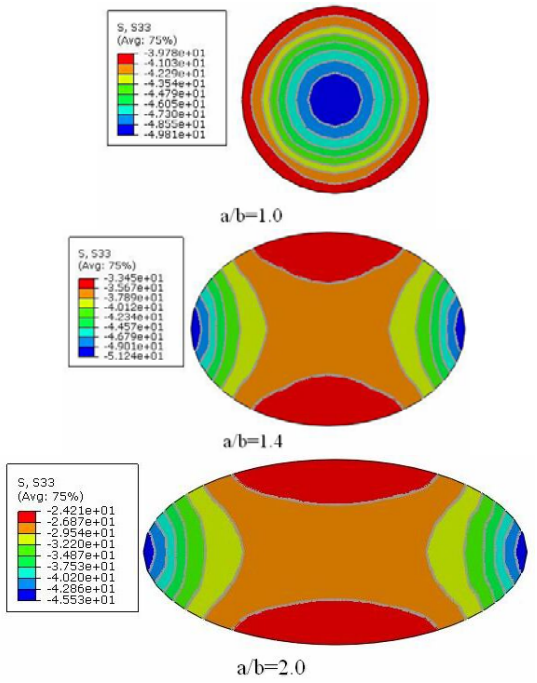

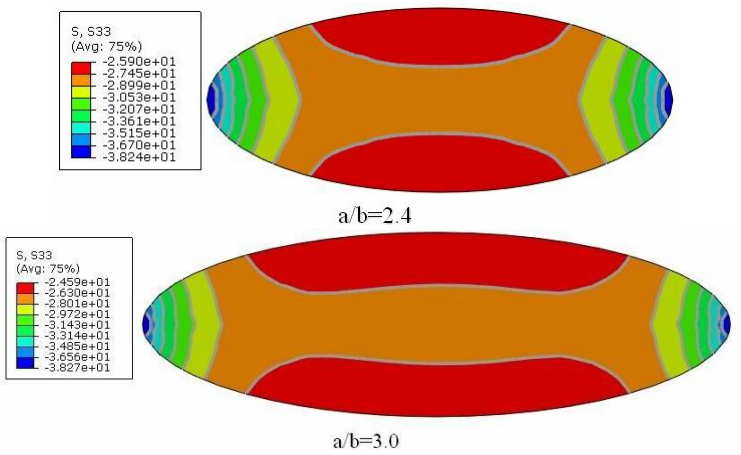

Figure 11. Stress Contour for Core Concrete

4. AXIAL COMPRESSIVE STRENGTH FORMULA FOR CFEST SHORT COLUMNS

In reference [1], a unified formula of axial compressive strength for concrete filled circular steel tube (CFCST) short columns is proposed, as shown in Eq. 17.

$$f_{sc}^{k}=\frac{1+1.5k\xi}{1+\frac{A_s}{A_c}}f_{ck} \tag{17}$$

where A_s and A_c are cross-sectional areas of steel and concrete respectively, ξ is characteristic values for the confining factor, $\xi=\frac{f_y A_s}{f_{ck}A_c}$, f_y and f_{ck} are the characteristic values for the yield strength of steel and cylinder strength of concrete respectively. k is confining cross-section adjustment factor. In this paper, by changing the elliptical cross section aspect ratios (a/b), the relation between k and a/b is studied.

According to previous theoretical analysis and finite element simulation results, it is assumed that stress distribution of the core concrete of CFEST is described by mathematical model as shown in Figure 12 [17-19]. The shaded area is effective distribution zone of lateral pressure, which consists of the surrounded area by two parabola lines c_1, c_2, and ellipse. The parabolic lines c_1 and c_2 are tangential to straight line y_1 and y_2 at the intersected points y_1, y_2 and ellipse, i.e. A, B, C and D. As the parabola lines c_1 and c_2 are symmetric to X axis, straight line y_1 and y_2 are symmetric to X and Y axis, only the position of A is required in order to determine the core concrete compressive area.

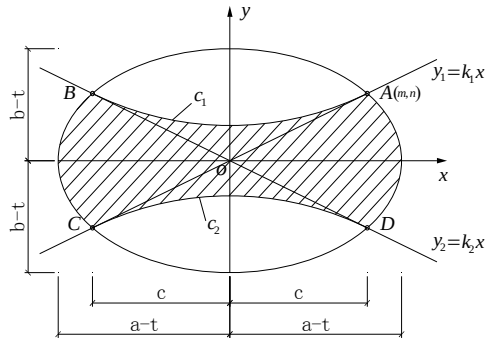

h

Figure 12. Effective Confining Area of Core Concrete

According to the parabola C_1 and the straight line Y_1 are tangent at A(m, n), simultaneous equations can be solved:

$$\left.\begin{array}{l}\dfrac{x^2}{(a-t)^2}+\dfrac{y^2}{(b-t)^2}=1\\ y=y_1=k_1x\end{array}\right\}\Rightarrow\begin{cases}m=x=\dfrac{1}{\sqrt{\dfrac{1}{(a-t)^2}+\dfrac{k_1^2}{(b-t)^2}}}\\ n=k_1m=\dfrac{k_1}{\sqrt{\dfrac{1}{(a-t)^2}+\dfrac{k_1^2}{(b-t)^2}}}\end{cases}\tag{18}$$

Parabola C_1 is expressed by $y=\frac{n}{2m^2}x^2+\frac{n}{2}$, and after integration, the compressive area of the core concrete can be obtained as follows：

$$\begin{aligned}A_{unconfined}&=4(a-t)(b-t)\left[\frac{m}{2(a-t)}\sqrt{1-\left(\frac{m}{a-t}\right)^2}\right.\\&\left.+\frac{1}{2}\arcsin\left(\frac{m}{a-t}\right)\right]-\frac{8mn}{3}\end{aligned}\tag{19}$$

$$\begin{aligned}A_{confined}&=\pi(a-t)(b-t)-A_{non-confined}\\&=\pi(a-t)(b-t)-4(a-t)(b-t)\left[\frac{m}{2(a-t)}\sqrt{1-\left(\frac{m}{a-t}\right)^2}\right.\\&\left.+\frac{1}{2}\arcsin\left(\frac{m}{a-t}\right)\right]+\frac{8mn}{3}\end{aligned}\tag{20}$$

$$\begin{aligned}k&=\frac{A_{confined}}{\pi(a-t)(b-t)}\\&=1-\frac{4\left[\dfrac{m}{2(a-t)}\sqrt{1-\left(\dfrac{m}{a-t}\right)^2}+\dfrac{1}{2}\arcsin\left(\dfrac{m}{a-t}\right)\right]}{\pi}+\frac{8mn}{3\pi(a-t)(b-t)}\end{aligned}\tag{21}$$

Based on the fact that the compressive lateral pressure is circlewise uniform for concrete filled circular steel tube, and according to regression analysis of finite element simulations, the relation between slope of straight line y_1 and a/b is as follows:

$$k_1=\frac{1}{\left(\dfrac{a}{b}\right)-1}\tag{22}$$

Putting Eq. 22 into Eq. 18, we have：

$$m=\frac{1}{\sqrt{\frac{1}{(a-t)^2}+\frac{b^2}{(a-b)^2(b-t)^2}}}$$
$$n=\frac{b}{(a-b)\sqrt{\frac{1}{(a-t)^2}+\frac{b^2}{(a-b)^2(b-t)^2}}} \tag{23}$$

Considering $t<<a,\ t<<b$, then $a-t\approx a,\ b-t\approx b$, and we have:

$$k=1-\frac{4\left[\frac{m}{2a}\sqrt{1-\left(\frac{m}{a}\right)^2}+\frac{1}{2}\arcsin\left(\frac{m}{a}\right)\right]}{\pi}+\frac{8mn}{3\pi ab} \tag{24}$$

$$m=\frac{1}{\sqrt{\frac{1}{a^2}+\frac{1}{(a-b)^2}}},\ n=\frac{b}{(a-b)\sqrt{\frac{1}{a^2}+\frac{1}{(a-b)^2}}} \tag{25}$$

In this paper, the cross sections for concrete filled elliptical steel tube are mainly with change of a/b at value 1.0 to 3.0. Through Eq. 25 into 21, we obtain the change of k to the change of a/b. As shown in Figure 13, k is a power function of a/b. After regression, we obtain $k=(a/b)^{-0.3}$.

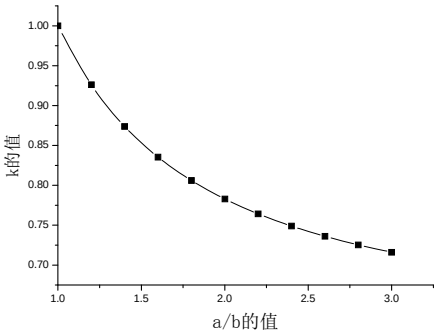

Figure 13. Confining Factor k against a/b

Therefore, axial compression formula for concrete filled elliptical steel tube short columns is as follows:

$$f_{sc}^{y}=\frac{1+1.5\left(\frac{b}{a}\right)^{0.3}\xi}{1+\frac{A_s}{A_c}}f_{ck} \tag{26}$$

5. EXPERIMENTAL VERIFICATION

Totally six axial compression tests for CFEST short columns were performed in Shenzhen Key Laboratory of Disaster Prevention and Mitigation HIT Shenzhen Graduate School. The specimens are divided into two groups, and the two groups adopt the same type of steel and concrete. The characteristic value for axial compressive strength of concrete is f_{ck}=22.0N/mm^2, and steel yield strength f_y=321N/mm^2. The specimen ID, geometrical sizes, and number are shown in Table 1. The setup of the specimens for the 1st group is shown in Figure 14, where the measurement locations are focused in the middle height since the end effect is smaller in these locations. The loading device is YAS-5000 electro-hydraulic servo universal testing machine, with the loading controlled by GTC350 all-digital electro-hydraulic servo controller. The specimens' top and bottom ends are both pin supported. The displacement control is used for loading, with a constant loading speed of 4kN/s.

Table 1. Geometrical Sizes and Number for CFEST Specimens

Group	ID	Cross section shape factor a/b	Geometrical size $(2a\times 2b\times t\times L)$ (mm×mm×mm×mm)
1	TY2.0-1	2.0	284×142×6×700
	TY2.0-2	2.0	284×142×6×700
	TY2.0-3	2.0	284×142×6×700
2	TY2.5-1	2.5	300×120×6×700
	TY2.5-2	2.5	300×120×6×700
	TY2.5-3	2.5	300×120×6×700

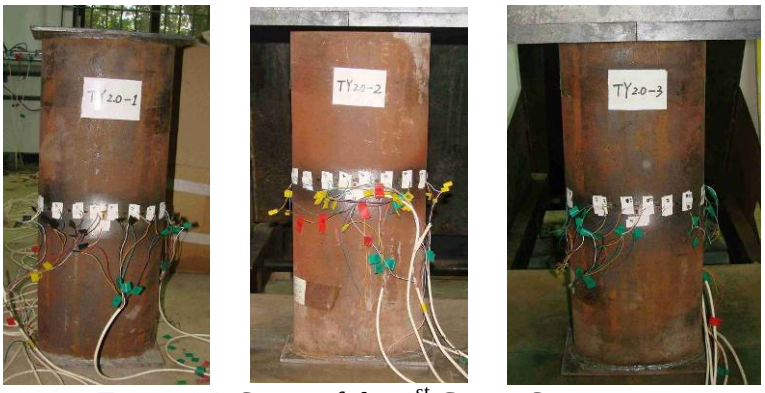

Figure 14. Setup of the 1st Group Specimens

Figure 15 (a) and Figure 15 (b) show load-displacement curves for CFEST short columns for the 1st and 2nd groups respectively. It can be seen from Figure 15 that all the specimens exhibit initial elastic stage, followed by a peak, and with further loading the specimens exhibit crisp or ductile behavior, i.e. the specimens TY2.0-2，TY2.5-1 and TY2.5-2 all exhibit sudden decrease after the peak stress state (crisp behavior), while the specimens TY2.0-1，TY2.0-3 and TY2.5-3 show gradual decrease after the peak, followed by increase again. This is because during the experiments, load eccentricity is relatively larger for the specimens TY2.0-2，TY2.5-1 and TY2.5-2. The increase for TY2.0-1，TY2.0-3 and TY2.5-3 is due to the fact the confining effect of the steel tube to concrete becomes stronger, leading to the increase of load-displacement curve.

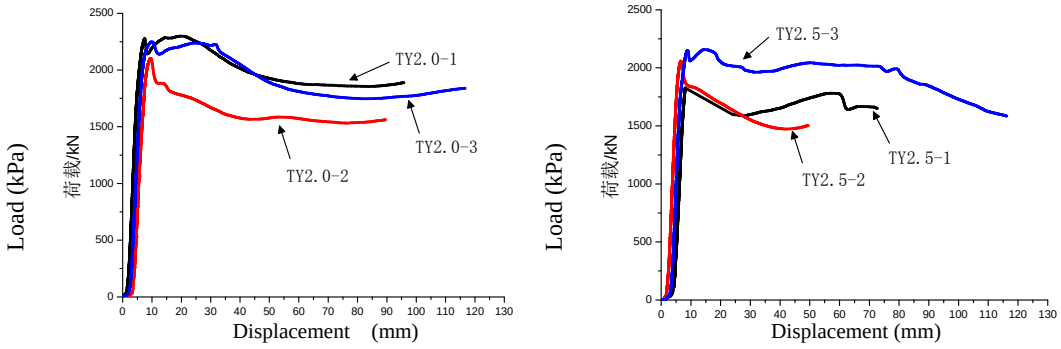

Figure 15. Load-displacement Curves for CFEST Short Columns

Figure 16 shows the pictures for the behavior of the specimens after loading of the concrete filled elliptical steel tube short columns for the 1st and 2nd groups respectively.

Figure 16. Behavior of the Specimens after Loading of the CFEST Short Columns

Table 2 is for test results, and table 3 is for comparison of test results and the formula-based results. Other test results are compared in Table 4. It can be seen from the table 3 and 4 that the calculated values are in good agreement with experimental results.

Table 2. Ultimate Compressive Capacity and Combined Compressive Strength

ID	Composite cross section area A_{sc} (mm^2)	Ultimate compressive capacity N_u (kN)	Combined compressive strength f_{sc} (N/mm^2)
TY2.0-1	31673.54	2299.00	72.62
TY2.0-2	31673.54	2102.00	66.40
TY2.0-3	31673.54	2249.00	71.04
TY2.5-1	28274.33	1827.00	64.65
TY2.5-2	28274.33	2059.00	72.86
TY2.5-3	28274.33	2157.00	76.33

Table 3. Comparison of Test Results and the Formula-based Results

Group	Formula based f_{sc}(N/mm^2)	Formula calculated N_u(kN)	Experimental averaged N_u(kN)	(Formula value) / (experimental value)
1	68.25	2161.75	2216.67	0.975
2	69.52	1965.76	2014.33	0.976

Table 4. Comparison of other Test Results and the Formula-based Results

Ref.	Group	Formula based f_{sc}(N/mm^2)	Formula calculated N_u(kN)	Experimental averaged N_u(kN)	(Formula value) / (experimental value)
[2-3]	150X75X4-C30 .NG/	94.94	847.82	839	1.011
	150X75X4-C60 .NG/	111.07	991.90	974	1.018
	150X75X4-C100 .NG/	140.87	1259.11	1265	0.995
	150X75X5-C30 .NG/	108.12	964.37	981	0.983
	150X75X5-C60 .NG/	122.81	1097.51	1084	1.012
	150X75X5-C100 .NG/	151.73	1355.17	1296	1.046
	150X75X6.3-C30 .NG/	136.18	1200.59	1193	1.006
	150X75X6.3-C60 .NG/	152.31	1346.03	1280	1.052
	150X75X6.3-C100 .NG/	176.55	1562.28	1483	1.053
	150X75X4-C30 .G/	95.50	849.64	780	1.089
	150X75X4-C60 .G/	111.70	997.84	961	1.038
	150X75X4-C100 .G/	141.49	1259.90	1272	0.990
	150X75X5-C30 .G/	107.82	965.67	988	0.977
	150X75X5-C60 .G/	123.45	1102.61	1123	0.982
	150X75X6.3-C100 .G/	178.40	1579.59	1160	1.362
[20]	EHS1 – SCC-Full	128.70	1141.70	1075	1.062
	EHS2 – SCC-Full	133.28	1185.55	1163	1.019
	EHS3 – SCC-Full	152.32	1353.85	1310	1.033
	EHS4 – SCC-Full	119.50	1881.26	1598	1.177
	EHS5 – SCC-Full	133.18	2099.23	2068	1.015
	EHS6 – SCC-Full	150.22	2367.13	2133	1.110
	EHS7 – SCC-Full	161.75	2553.59	2290	1.115
	EHS8 – NC-Full	115.52	2216.68	2109	1.051

6. STABILITY FACTOR UNDER AXIAL COMPRESSION FOR CFEST LONG COLUMNS

For the concrete filled steel tube, based on unified theory with considering the composite to be one material, the stability factor can be calculated as follows [1]:

$$\varphi = \frac{1}{2\bar{\lambda}_{sc}^{\ 2}}\left\{\bar{\lambda}_{sc}^{\ 2} + (1+\varepsilon_{sc}) - \sqrt{\left[\bar{\lambda}_{sc}^{\ 2} + (1+\varepsilon_{sc})\right]^2 - 4\bar{\lambda}_{sc}^{\ 2}}\right\} \tag{27}$$

where slenderness ratio is defined as：

$$\bar{\lambda}_{sc} = \frac{\lambda}{\pi}\sqrt{\frac{f_{sc}}{E_{sc}}}$$

where ε_{sc} is the effective initial eccentricity of concrete filled steel tube and $\varepsilon_{sc} = K\bar{\lambda}_{sc}$; K is the initial eccentricity coefficient of concrete filled steel tube and $K = 0.25\alpha^N$; α is steel ratio, equal to the ratio of the steel section area and the composite section area $A_s/(A_s + A_c)$; N is cross section shape factor.

In calculating the stability factor, bending stiffness is used and the composite elastic modulus is calculated as follows:

$$E_{sc} = \frac{E_c I_c + E_s I_s}{I_{sc}} \tag{28}$$

In this paper, based on Eq. 27 and a number of finite element analysis, and after regression analysis, the stability factor for concrete filled elliptical steel tube short and long columns is as follows [11]:

$$\varphi = \frac{1}{2\overline{\lambda}_{sc}^{\,2}}\left\{\overline{\lambda}_{sc}^{\,2} + (1+\varepsilon_{sc}) - \sqrt{\left[\overline{\lambda}_{sc}^{\,2} + (1+\varepsilon_{sc})\right]^2 - 4\overline{\lambda}_{sc}^{\,2}}\right\} \tag{29}$$

$$\varepsilon_{sc} = K\overline{\lambda}_{sc} \tag{30}$$

$$K = 0.25\alpha^N \tag{31}$$

$$N = \left(\frac{a}{b}\right)^m \tag{32}$$

where a is half the length of long axis of elliptical cross section, b is half the length of short axis of elliptical cross section, $m = -6$ for action around long axis, $m = -2$ for action around short axis.

For the work reported a total of 198 finite element models are established [11]. Stability factor is analyzed for different parameters, as listed in table 4. Comparison of formula based value with the finite element results gives an average value of 1.021 and error variance is 0.002. This indicates that the formula can describe the stability capacity for CFEST long columns.

Table 4. Parameters for Axial Compressive Long Column

Parameter	Value
Steel yield strength f_y / MPa	235, 345, 90
Concrete axial compressive characteristic strength f_{ck} / MPa	20.1, 26.8, 32.4
Steel ratio a	0.098～0.160
Section shape a/b	1.0, 1.2, 1.4, 1.6, 1.8, 2.0, 2.2, 2.4, 2.6, 3.0
Length L / mm	1200, 2100, 3000

7. CONCLUDING REMARKS

This paper presents theoretical analysis of axial compressive behavior of concrete filled elliptical steel tube members. The theoretical analysis shows the distribution rule of interaction between steel tube and core concrete for CFEST column under axial compression based on limit equilibrium, which is verified by both experimental tests and finite element simulations. A unified axial compressive strength formula and stability factor are obtained for CFEST columns.

Appendix : Notations

$f_{lx}(x)$: lateral pressure of concrete along x when abscissa is x

$f_{ly}(y)$: lateral pressure of concrete along y when ordinate is y

$f_{ly}(0)$: lateral pressure of concrete along y when ordinate is 0

$f_{lx}(0)$: lateral pressure of concrete along x when abscissa is 0

$N(x)$: circumferential tension of steel tube when abscissa is x

N_1: circumferential tension of steel tube when abscissa is a

N_2: circumferential tension of steel tube when x=0

α: the angle between x axis and the tangential to the elliptic curve at x

$\sigma(x)$: circumferential tension of steel tube at x

σ_1: circumferential tension of steel tube at x=a

σ_2: circumferential tension of steel tube at x=0

f_{ck}: peak value of stress of concrete

ε_e: compressive strain of concrete corresponding to stress with the value of $0.3f_{ck}$ at hardening stage

ε_c: compressive strain of concrete corresponding to stress with the peak value of f_{ck}

ε_c: compressive strain of concrete corresponding to stress with the value of $0.5f_{ck}$ at softening stage

α_a, α_d - model constants for concrete

G_f: fracture energy required to cause one continuous crack per unit area

σ_{t0}: failure stress of concrete

f_p: proportional limit value of steel

f_y: characteristic yield strength value of steel

f_u: ultimate strength value of steel

E_s: Young's modulus of elasticty

$\varepsilon_e = 0.8f_y / E_s$

$\varepsilon_{e1} = 1.5\varepsilon_e$

$\varepsilon_{e2} = 10\varepsilon_{e1}$

$\varepsilon_{e3} = 100\varepsilon_{e1}$

A: model constant for steel , $A = 0.2f_y / (\varepsilon_{e1} - \varepsilon_e)^2$,

B: model constant for steel, $B = 2A\varepsilon_{e1}$

C: model constant for steel, $C = 0.8f_y + A\varepsilon_e^{\ 2} - B\varepsilon_e$.

e_0: initial eccentricity

A_s: cross-sectional areas of steel

A_c: cross-sectional areas of concrete

ξ: characteristic values for the confining factor, $\xi = \dfrac{f_y A_s}{f_{ck} A_c}$

f_{ck}: characteristic values for cylinder strength of concrete

k: confining cross-section adjustment factor

ε_{sc}: effective initial eccentricity of concrete filled steel tube and $\varepsilon_{sc} = K\overline{\lambda}_{sc}$

K : initial eccentricity coefficient of concrete filled steel tube and $K = 0.25\alpha^N$
α : steel ratio, equal to $A_s/(A_s + A_c)$
A_s : section area of steel
A_c : section area of concrete
N : cross section shape factor
a: half length of long axis of elliptical cross section
b : half length of short axis of elliptical cross section
a/b: aspect ratio
E_{sc} : composite (steel and concrete) elastic modulus
E_c : elastic modulus of concrete
I_c : area moment of inertia for concrete
E_s : Young's modulus of elasticty
I_s : area moment of inertia for steel
I_{sc} : area moment of inertia for concrete and steel

REFERENCES

[1] Yu, M., Zha, X.X., Ye, J. and She, C.Y., "A Unified Formulation for Hollow and Solid Concrete-filled Steel Tube Columns under Axial Compression", Engineering Structures, 2010, Vol. 32, No. 4, pp. 1046-1053.
[2] Manojkumar V. Chitawadagi, and Mattur C. Narasimhan1, "Strength Deformation Behavior of Circular Concrete Filled Steel Tubes Subjected to Pure Bending", Journal of Constructional Steel Research, 2009, Vol. 65, pp. 1836-1845.
[3] Yang, H., Lam, D. and Gardner, L., "Testing and Analysis of Concrete-filled Elliptical Hollow Sections", Engineering Structures, 2008, Vol. 30, No. 2, pp. 3771-3781.
[4] Dai, X. and Lam, D., "Numerical Modelling of the Axial Compressive Behavior of Short Concrete-filled Elliptical Steel Columns", Journal of Constructional Steel Research, 2010, Vol. 66, No. 7, pp. 931-942.
[5] Guo, L, Zhang, S, Kim, W. and Ranzi, G., "Behavior of Square Hollow Steel Tubes and Steel Tubes Filled with Concrete", Thin-Walled Structures, 2007, Vol. 45, pp. 961-973.
[6] Varma, A.H., Ricles, J.M., Sause, R. and Lu, L.W., "Experimental Behavior of High Strength Square Concrete-Filled Steel Tube Beam-Columns", Journal of Structural Engineering, ASCE. 2002, Vol. 128, No. 3, pp. 309-318.
[7] Chen, B.C., Ou, Z.Q., Wang, L.Y. and Han, L.H., "Eccentric Bearing Capacity Analysis of Concrete Filled Steel Tube", 2002, Vol. 30, No. 6, pp. 838-844. (in Chinese)
[8] Yu, Z.W. and Ding, X.F., "Mechanical Properties.of Concrete Filled Circular Steel Tube Eccentric Loaded Columns", 2008, Vol. 21, No. 1, pp. 40-46. (in Chinese)
[9] Toshiaki Fujimoto, Akiyoshi Mukai, Isao Nishiyama and Kenji Sakino, "Behavior of Eccentrically Loaded Concrete-Filled Steel Tubular Columns", Journal of Structural Engineering, ASCE. 2004, Vol. 130, No. 2, pp. 203-212.
[10] Zhong, S.T., "Unified Theory of Concrete Filled Steel Tube - Theoretical Research and Application", Tsinghua University Press, 2006. (in Chinese)
[11] Liu, X.C., "Study of Basic Properties of Concrete Filled Elliptical Steel Tube", Master Thesis, Harbin Institute of Technology Shenzhen Graduate School, 2010, Vol. 6. (in Chinese)
[12] ABAQUS Analysis User's Manual, Volume III: Materials, SIMULIA.

[13] GB50010-2002, Code for Design of Xoncrete Structures", Ministry of Construction, People's Republic of China. (in Chinese)
[14] Yao, G.H., "Research on Behaviour of Mechanism of Concrete-filled Steel Tubes Subjected to Complicated Loading States", PhD Thesis, Fuzhou University, 2006. (in Chinese)
[15] Han, L.H., "Concrete Filled Steel Tube Structure - Theory and Practice", Science Press, 2004. (in Chinese)
[16] GB50205-2001, Code for Acceptance of Construction Quality of Steel Structures", Ministry of Construction, People's Republic of China. (in Chinese)
[17] Tan, T.H. and Yip, W.K., "Behavior of Axially Loaded Concrete Columns Confined by Elliptical Hoops", ACI Structural Journal, 1999, Vol. 96, No. 6, pp. 967-973.
[18] Chung, H.S., Yang, K.H., Lee, Y.H. and Eun, H.C.," Stress–strain Curve of Laterally Confined Concrete", Engineering Structures, 2002, Vol. 24, No. 9, pp. 1153-1163.
[19] Razvi, S. and Saatcioglu, M., "Confinement Model for High-strength Concrete", ASCE, Journal of Structural Engineering, 1999, Vol. 125, No. 3, pp. 281-289.
[20] Zhao, X.L. and Packer, J.A., "Tests and Design of Concrete-filled Elliptical Hollow Section Stub Columns", Thin-Walled Structures, 2009, Vol. 47, pp. 617-628.